Bayesian and Empirical Bayesian Forests

Abstract

We derive ensembles of decision trees through a nonparametric Bayesian model, allowing us to view such ensembles as samples from a posterior distribution. This insight motivates a class of Bayesian Forest (BF) algorithms that provide small gains in performance and large gains in interpretability. Based on the BF framework, we are able to show that high-level tree hierarchy is stable in large samples. This motivates an empirical Bayesian Forest (EBF) algorithm for building approximate BFs on massive distributed datasets and we show that EBFs outperform subsampling based alternatives by a large margin.

1. Introduction

Decision trees are a fundamental machine learning tool. They partition the feature (input) space into regions of response homogeneity, such that the response (output) value associated with any point in a given partition can be predicted from the average for that of neighbors. The classification and regression tree (CART) algorithm of (Breiman et al., 1984) is a common recipe for building trees; it grows greedily through a series of partitions on features, each of which maximizes reduction in some measure of impurity at the current tree leaves (terminal nodes; i.e., the implied input space partitioning). The development of random forests (RF) by (Breiman, 2001), which predict through the average of many CART trees fit to bootstrap data resamples, is an archetype for the successful strategy of tree ensemble learning. For prediction problems with training sets that are large relative to the number of inputs, properly trained ensembles of trees can predict out-of-the-box as well as any carefully tuned, application-specific alternative.

This article makes three contributions to understanding and application of decision tree ensembles (or, *forests*).

Bayesian forest: A nonparametric Bayesian (npB) point-of-view allows for the straightforward, but not well-recognized, interpretation of forests as a sample from a posterior over trees. Imagine CART applied to a data generating process (DGP) with finite support: the tree greedily splits support to minimize impurity of the partitioned response distributions (terminating at some minimum-leaf-probability threshold). We present a nonparametric Bayesian model for DGPs based on multinomial draws from (large) finite support, and derive the Bayesian forest (BF) algorithm for sampling from the distribution of CART trees implied by the posterior over DGPs. Random forests are an approximation to this BF exact posterior sampler, and we show in examples that BFs provide a small but reliable gain in predictive performance over RFs.

Posterior tree variability: Based upon this npB framework, we derive results on the approximate stability of CART over different DGP realizations. In particular, we find that, for the data at a given node on the sample CART tree, the probability that the next split for a posterior DGP realization matches the sample split location is

$$\mathrm{p}\left(\text{split matches sample CART}\right) \gtrsim 1 - \frac{p}{\sqrt{n}} e^{-n}, \qquad (1)$$

where p is the number of possible split locations and n the number of observations on the current node. Even if p grows with n, the result indicates that partitioning can be stable conditional on the data being split. This conditioning is key: CART's well known instability is due to its recursive nature, such that a single split different from sample CART at some node removes any expectation of similarity below that node. However, for large samples, (1) implies that we will see little variation at the top hierarchy of trees in a forest. We illustrate such stability in our examples.

Empirical Bayesian forests for Big Data: the npB forest interpretation and tree-stability results lead us to propose empirical Bayesian forests (EBF) as an algorithm for building approximate BFs on massive distributed datasets (e.g., those stored on a Hadoop distributed file system). Traditional empirical Bayesian analysis fixes parameters in high levels of a hierarchical model at their marginal posterior mode, and proceeds to quantify uncertainty for the rest of the model conditional upon these fixed values. EBFs work the same way: we fit a single shallow CART *trunk* to the sample data, and then sample a BF ensemble of *branches* at each terminal node of this trunk. The initial CART trunk thus maps observations to their branch, and each branch BF can be fit in parallel without any communication with

Preliminary work. Under review by the International Conference on Machine Learning (ICML). Do not distribute.

the other branches. When we expect little posterior variability about the trunk structure, an EBF sample should look similar to the (much more costly, or even infeasible) full BF sample. In a number of experiments, we compare EBFs to the common distributed-computing strategy of fitting forests to random data subsets, and find that the EBFs lead to a large improvement in predictive performance.

BFs offer small performance advantages over RFs, but their main usefulness is as a Bayesian interpretation for ensembles of CART trees. The intuition gained is especially valuable because there is little frequentest theory available on inference for decision trees. The BF model also motivates the more practical contribution of EBFs, leading to new algorithms for distributed computing and cost savings from avoiding repeatedly sampling model levels about which you have little uncertainty. This type of strategy is the key to efficient machine learning with Big Data: focus the 'Big' on the pieces of models that are most difficult to learn.

Bayesian forests are introduced in Section 2 along with a survey of Bayesian tree models, Section 3 investigates tree stability in theory and practice, and Section 4 presents the empirical Bayesian forest framework. Throughout, we use publicly available data on home prices in California to illustrate our ideas. We also provide a variety of other data analyses to benchmark performance, and close with description of how EBF algorithms are being built and perform in large-scale machine learning at eBay.com.

2. Bayesian forests

Informally, write dgp to represent the random variable defined over an as-of-yet undefined set of possible DGPs. A Bayesian analogue to classical 'distribution-free' nonparametric statistical analysis (e.g., Hollander & Wolfe, 1999) has two components:

1. set a nonparametric statistic $\mathcal{T}(dgp)$ that is of interest in your application regardless of the true DGP,
2. and build a flexible model for the DGP, so that the posterior distribution on $\mathcal{T}(dgp)$ can be derived from posterior distribution on possible DGPs.

In the context of this article, $\mathcal{T}(dgp)$ refers to a CART tree. Indeed, trees are useful precisely because they are good predictors regardless of the underlying data distribution – they do not rely upon distributional assumptions to share information across training observations. Our DGP model, detailed below, leads to a posterior for dgp that is represented through random weighting of observed support. A Bayesian forest contains CART fits corresponding to each draw of support weights, and the BF ensemble prediction is an approximate posterior mean.

2.1. Nonparametric model for the DGP

We employ a Dirichlet-multinomial sampling model in nonparametric Bayesian analysis. The approach dates back to Ferguson (1973). Chamberlain & Imbens (2003) provide an overview in the context of econometric problems. Rubin (1981) proposed the Bayesian bootstrap as an algorithm for sampling from versions of the posterior implied by this strategy, and the algorithm has since become closely associated with this model.

Use $\mathbf{z}_i = \{\mathbf{x}_i, y_i\}$ to denote the features and response for observation i. We suppose that data are drawn *independently* from a finite L possible values,

$$dgp = \mathrm{p}(\mathbf{z}) = \sum_{l=1}^{L} \omega_l \mathbb{1}_{[\mathbf{z}=\boldsymbol{\zeta}_l]} \tag{2}$$

where $\omega_l \geq 0 \forall l$ and $\sum_l \omega_l = 1$. Thus the generating process for observation i draws l_i from a multinomial with probability ω_{l_i}, and this indexes one of the L support points. Since L can be arbitrarily large, and all data are stored as discrete, this so-far implies no restrictive assumptions beyond that of independence.

The conjugate prior for $\boldsymbol{\omega}$ is a Dirichlet distribution, written $\mathrm{Dir}(\boldsymbol{\omega};\boldsymbol{\nu}) \propto \prod_{l=1}^{L} \omega_j^{\nu_l - 1}$. We will parametrize the prior with a single concentration parameter $\boldsymbol{\nu} = a > 0$, such that $\mathbb{E}[\omega_l] = a/La = 1/L$ and $\mathrm{var}(\omega_l) = (L-1)/[L^2(La+1)]$. Suppose you have the observed sample $\mathbf{Z} = [\mathbf{z}_1 \cdots \mathbf{z}_n]'$. For convenience, we allow $\boldsymbol{\zeta}_l = \boldsymbol{\zeta}_k$ for $l \neq k$ in the case of repeated values. Write $l_1 \ldots l_n = 1 \ldots n$ so that $\mathbf{z}_i = \boldsymbol{\zeta}_i$ and $\mathbf{Z} = [\boldsymbol{\zeta}_1 \cdots \boldsymbol{\zeta}_n]'$. Then the posterior distribution for $\boldsymbol{\omega}$ has $\omega_i = a + 1$ for $i \leq n$ and $\omega_l = a$ for $l > n$, so that

$$\mathrm{p}(\boldsymbol{\omega}) \propto \prod_{i=1}^{n} \omega_i^a \prod_{l=n+1}^{L} \omega_l^{a-1}. \tag{3}$$

This, in turn, defines our posterior for the data generating process through our sampling model in (2).

There are many possible strategies for specification of a and ζ_l for $l > n$.[1] The non-informative prior that arises as $a \to 0$ is a convenient default: in this limit, $\omega_l = 0$ with probability one for $l > n$.[2] We apply this limiting prior throughout, such that our posterior for the data generating process is a multinomial draw from the observed data points, with a uniform $\mathrm{Dir}(\mathbf{1})$ distribution on the $\boldsymbol{\omega} = [\omega_1 \ldots \omega_n]'$ sampling probabilities. We will also find it convenient to parametrize un-normalized $\boldsymbol{\omega}$ via IID exponential random variables: $\boldsymbol{\theta} = [\theta_1 \ldots \theta_n]$, where $\theta_i \overset{ind}{\sim} \mathrm{Exp}(1)$ in the posterior and $\omega_i = \theta_i/|\boldsymbol{\theta}|$ with $|\boldsymbol{\theta}| = \sum_i \theta_i$.

[1] The unobserved ζ_l act as data we imagine we might have seen, to smooth the posterior away from the data we have actually observed. See Poirier (2011) for discussion.

[2] For $l > n$ the posterior has $\mathbb{E}[\omega_l] = 0$ with variance $\mathrm{var}(\omega_l) = \lim_{a\to 0} a[n+a(L-1)]/[(n+La)^2(n+La+1)] = 0$.

2.2. CART as posterior functional

Conditional upon $\boldsymbol{\theta}$, the population tree $\mathcal{T}(dgp)$ is defined through a weighted-sample CART fit. In particular, given data $\mathbf{Z}^\eta = \{\mathbf{X}^\eta, \mathbf{y}^\eta\}$ in node η, sort through all dimensions of all observations in $\mathbf{Z}^\eta$ to find the split that minimizes the average of some $\boldsymbol{\omega}$-weighted impurity metric across the two new child nodes. For example, in the case of regression trees, the impurity to minimize is weighted-squared error

$$\mathcal{I}(\mathbf{y}^\eta) = \sum_{i \in \eta} \theta_i (y_i - \mu_\eta)^2 \tag{4}$$

with $\mu_\eta = \sum_i \theta_i y_i / |\boldsymbol{\theta}^\eta|$. The split candidates are restricted to satisfy a minimum leaf probability, such that every node in the tree must have $|\boldsymbol{\theta}^\eta|$ greater than some threshold.[3] This procedure is repeated on every currently-terminal tree node until it is no longer possible to split while satisfying the minimum probability threshold. To simplify notation, we refer to the resulting CART tree as $\mathcal{T}(\boldsymbol{\theta})$.

2.3. Posterior sampling

Following (Rubin, 1981) we can obtain a sample from the posterior on $\mathcal{T}(\boldsymbol{\theta})$ through a simple Bayesian bootstrap.

Algorithm 1 Bayesian Forest

for $b = 1$ **to** B **do**
  draw $\boldsymbol{\theta}^b \overset{iid}{\sim} \text{Exp}(\mathbf{1})$
  run weighted-sample CART to get $\mathcal{T}_b = \mathcal{T}(\boldsymbol{\theta}^b)$
end for

We've implemented BF through simple adjustment of the `ensemble` module of python's `scikit-learn` (Pedregosa et al., 2011).[4] As a quick illustration, Figure 1 shows three fits for the conditional mean for velocity of a motorcyle helmet after impact in a crash: sample CART $\mathcal{T}(\mathbf{1})$, a single draw of $\mathcal{T}(\boldsymbol{\theta}^b)$, and the BF average prediction (data are from Venables & Ripley, 2002).

Note that the Bayesian forest differs from Breiman's random forest only in that the weights are drawn from an exponential (or Dirichlet, when normalized) distribution rather than a Poisson (or multinomial) distribution. To the extent that RF sampling provides a coarse approximation to the BF samples, the former is a convenient approximation. Moreover, we will find little difference in predictive performance between BFs and RFs, so that one should feel free to use readily available RF software while still relying on the ideas of this paper for intuition and interpretation.

[3] In practice this can be replaced with a threshold on the minimum number of observations at each leaf.

[4] Replace the variable `sample_counts` in `forest.py` to be drawn exponential rather than binomial when bootstrapping.

2.4. Bayesian tree-as-parameter models

Other Bayesian analyses of DTs the tree as a parameter which governs the DGP, rather than a functional thereof, and thus place some set of restrictions on the distributional relationship between inputs and outputs.

The original Bayesian tree model is the Bayesian CART (BCART) of Chipman et al. (1998). BCART defines a likelihood where response values for observations allocated (via $\mathbf{x}$) to the same leaf node are IID from some parametric family (e.g., for regression trees, observations in each leaf are IID Gaussian with shared variance and mean). BCART is fit through Markov chain Monte Carlo (MCMC), drawing from the tree posterior by proposing a number of possible changes to current tree fit (e.g. grow or prune a given leaf node). A natural extension of this framework is to consider alternative leaf models. The BCART authors propose linear regression leaves, while the Treed Gaussian Processes (TGP) of Gramacy & Lee (2008) use Gaussian process regression at each leaf. As an alternative to MCMC, Taddy et al. (2011) proposed dynamic regression trees (dynaTree) fit through sequential Monte Carlo (SMC), allowing trees to grow naturally with streaming data through small updates to a particle cloud of trees. [5]

MCMC and SMC tree sampling use the same incremental moves that are familiar from CART. Unfortunately, this means that they tend to get stuck in locally-optimal regions of tree-space. As an alternative, the original BCART authors developed the Bayesian Additive Regression Trees Chipman et al. (BART; 2010) algorithm, which replaces a single tree parameter target with the sum of many small trees. An input vector is allocated to a leaf in each tree, and the corresponding response distribution has mean equal to the average of each leaf node value and variance equal to a single value that is shared across observations. Original BART assumes Gaussian response, and extensions include Gaussian mixtures. Since BART only ever samples very short trees, MCMC is fast and mixes well.

Easy sampling comes at a potentially steep price: the assumption of homoskedastic additive errors.[6] Despite this restriction, empirical studies have repeatedly shown BART to outperform alternative flexible prediction rules. Many response variables (especially after, say, log transformation) have the property that they are well fit by flexible regression with homoskedastic errors. Whenever the model assumptions in BART are close enough to true, it should outperform methods which do not make those assumptions. The same advantage holds for BCART, TGP, or dynaTree whenever their implied DGP assumptions are not invalid.

[5] Note that the Bayesian bootstrap is also a potential sampling tool in this tree-as-parameter setting. See Clyde & Lee (2001) for details on the technique and its relation to model averaging.

[6] For classification, this is manifest through a Probit link.

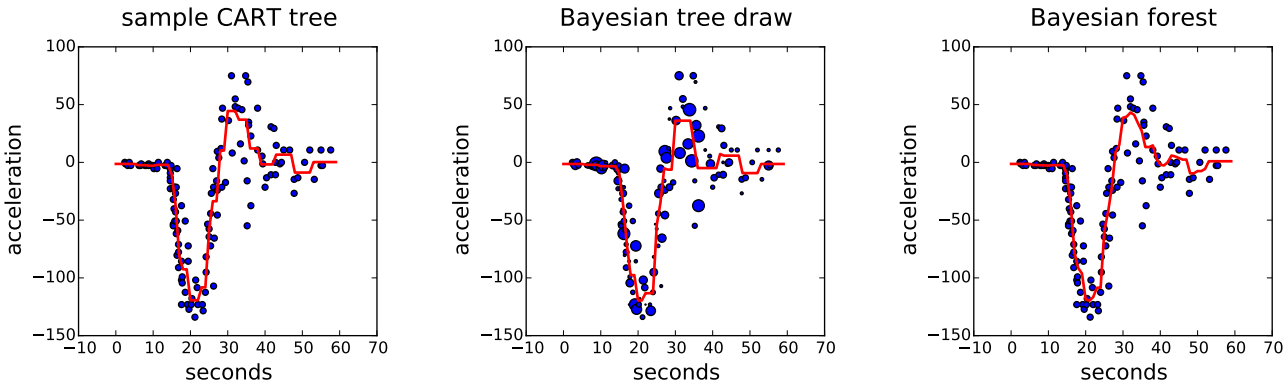

Figure 1. Motorcycle data illustration. The lines show each of CART fit to the data sample, CART fit to a sample with weights drawn IID from an exponential (point size proportional to weight), and the BF predictor which averages over 100 weighted CART fits.

In contrast, the npB interpretation of forests (BF or RF) makes it clear that they are suited to applications where the response distribution defies parametric representation, such that CART fit is the most useful DGP summary available. We often encounter this situation in application. For example, internet transaction data combines discrete point masses with an incredibly fat right tail (e.g., see Taddy et al., 2014). In academia it is common to transform such data before analysis, but businesses wish to target the response on the scale measured (e.g., clicks or dollars) and need to build a predictor that does well on that scale.

2.5. Friedman example

A common simulation experiment in evaluating flexible predictors is based around the Friedman (1991) function,

$$y = f(\mathbf{x}) + \varepsilon \qquad (5)$$
$$= 10\sin(\pi x_1 x_2) + 20(x_3 - 0.5)^2 + 10x_4 + 5x_5 + \varepsilon.$$

where $\varepsilon \sim \mathrm{N}(0,1)$ and $x_j \sim \mathrm{U}(0,1)$.

For our experiment, we follow previous authors by including as features for training the spurious $x_6 \ldots x_p$. Each regression models are fit to 100 random draws from (5) and tested at 1000 new $\mathbf{x}$ locations. Root mean square error (RMSE) is calculated between predicted and true $f(\mathbf{x})$.

Results over 100 repeats are shown in Figure 5.[7] As forecast, the only model which assumes the true homoskedastic error structure, BART, well outperforms all others. The two forests, BF and RF, are both a large improvement over

[7]In this and the next example, CART-based algorithms had minimum-leaf-samples set at 3 and the ensembles contain 100 trees. BART and BCART run at their `bayestree` and `tgp` R package defaults, except that BART draws only 200 trees after a burn-in of 100 MCMC iterations. This is done to get comparable compute times; for these settings BART requires around 75 seconds per fold with the California housing data, compared to BF's 10 seconds when run in serial, and 3 seconds running on 4 cores.

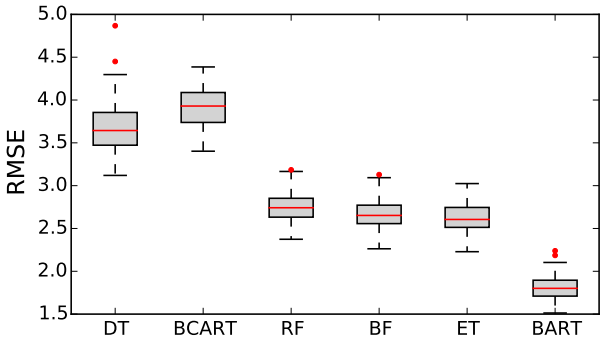

Figure 2. Friedman experiment predictive RMSE over 100 runs.

DT. The BF average RMSE is only about 1% better than the RF's, since Bayesian and classical bootstrapping differ little in practice. BCART does very poorly: worse than a single DT. We hypothesis that this is due to the notoriously poor mixing of the BCART MCMC, such that this fit is neither finding a posterior mean (as it is intended to) or optimizing to a local posterior mode (as DT does).

We also include the extremely random trees (ET) of Geurts et al. (2006), which are similar to RFs except that (a) instead of optimizing greedy splits, a few candidate splits are chosen randomly and the best is used and (b) the full unweighted data sample is used to fit each tree. ET slightly outperforms both BF and RF; in our experience this happens in small datasets where the restriction of population support to observed support (as assumed in our npB analysis) is invalid and the forest posteriors are over-fit.

2.6. California housing data

As more realistic example, we consider the California housing data of Pace & Barry (1997) consisting of median home price along with eight features (location, income,

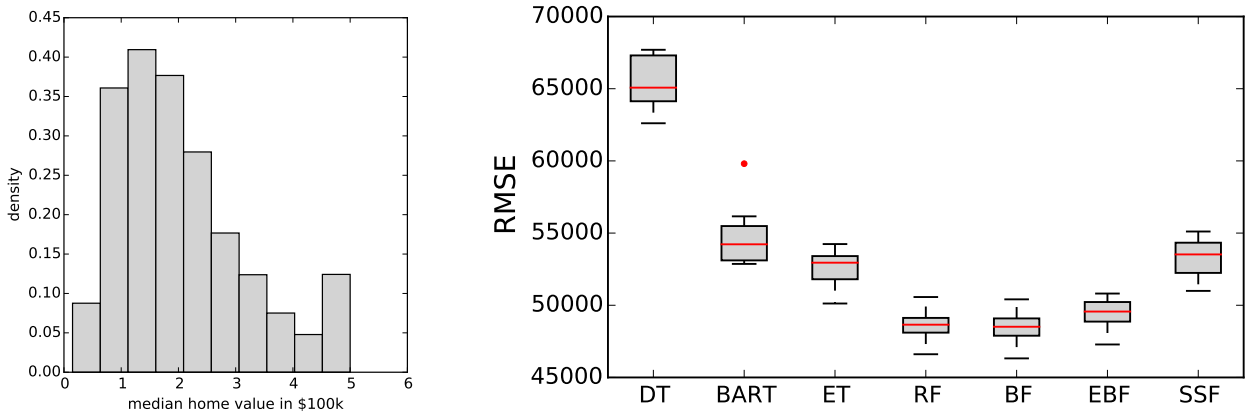

Figure 3. California housing data. The response sample is on the left, and the right panel shows predictive RMSE across 10-fold CV.

housing stock) for 20640 census blocks. Since prices tend to vary with covariates on a multiplicative scale, standard analyses take log median price as the response of interest. Instead, we will model the conditional expectation of dollar median price. This is relevant to applications where prediction of raw transaction data is of primary interest. The marginal response distribution for median home price is shown in the left panel of Figure 3.[8]

Figure 3 shows results from a 10-fold cross-validation (CV) experiment, with details in Table 1. Except for DT and BCART, which still perform worse than all others[9], results are reversed from those for the small-sample and homoskedastic Friedman data. Both RF and BF do much better than BART and it's restrictive error model. BF again offers a small gain over RF. Since the larger sample size makes observed support a better approximation to population support, the forests outperform ET. The EBF (empirical Bayesian forest) and SSF (sub-sample forest) predictors are based on distributed computing algorithms that we introduce later in Section 3. At this point we note only that the massively scalable EBF is amongst the top performers; the next section helps explain why.

	BF	RF	EBF	ET	SSF	BART	DT
RMSE	48.2	48.5	49.4	52.5	53.1	54.8	65.6
%WTB	0.0	0.5	2.4	8.7	10.0	13.4	35.9

Table 1. Average RMSE in $10k and % worse-than-best for the California housing data 10-fold CV experiment.

3. Understanding the posterior over trees

Theory on decision trees is sparse. The original CART book of (Breiman et al., 1984) provides results on asymptotic consistency; they show that any partitioner that is able to eventually learn enough to split the DGP support into very small probability leaves will be able to reproduce the conditional response distribution of that DGP. However, this result says nothing about the structure of the underlying trees, nor does it say anything about the ability of a tree to predict when there is not enough data to finely partition the DGP. Others have focused on the frequentest properties of individual split decisions. In the original CHAID work of (Kass, 1980), splits are based upon χ^2 tests at each leaf node. (Loh, 2002) and (Hothorn et al., 2006) are example generalizations, both of which combat the multiple testing and other biases inherent in tree-building through a sequence of hypothesis tests. However, such contributions provide little intuition about the variability of an entire decision tree or in the setting where we are not working from a no-split null hypothesis distribution.

Despite this lack of theory, it is generally accepted that in practice there is usually large uncertainty (sampling or posterior) about the structure of decision trees. For example, (Geurts & Wehenkel, 2000) present extensive simulation of tree uncertainty. They find that the locations and order of split points in trees is sometimes no-better than random (indeed, this motivates work by the same authors on extremely random trees). The intuition behind such randomness is clear: the probability of a tree having any given branch structure is the product of conditional probabilities for each successive split. After a enough steps any specific tree approaches probability of zero.

However, it is possible that elements of the tree structure are fairly stable. For example, in the context of boosting, (Appel et al., 2013) argue that the conditionally optimal split locations for internal nodes can be learned from subsets of the full data allocated to each node, and they use this to propose a faster boosting algorithm. In this section we make a related claim: in large samples, there is little pos-

[8] Values appear to have been capped at $500k

[9] We've left off BCART's average RMSE of $82k, 70% WTB.

terior variation for the top of the tree. We make this point first in theory, then through empirical demonstration.

3.1. Probability of the sample CART tree

We focus on regression trees for this derivation, wherein node impurity is measured as the sum of squared errors. Consider a simplified setup with each $x_j \in \{0, 1\}$ a binary random variable (possibly created through discretization of a continuous input). We'll investigate here the probability that the impurity minimizing split on a given node is the same for a given realization of posterior DGP weights as it is for the unweighted data sample.

Suppose $\{\mathbf{z}_1 \dots \mathbf{z}_n\}$ are the data to be partitioned at some tree node, with $\mathbf{z}_i = [y_i, x_{i1}, \dots, x_{ip}]'$. Say that $\mathtt{f}_j = \{i : x_{ij} = 0\}$ and $\mathtt{t}_j = \{i : x_{ij} = 1\}$ are the partitions implied by splitting on a given x_j. The resulting impurity is

$$\sigma_j^2(\boldsymbol{\theta}) = \frac{1}{n} \sum_i \theta_i \left[y_i - \mu_j(x_{ij}) \right]^2, \tag{6}$$

$\mu_j(0) = \sum_{i \in \mathtt{f}_j} y_i \, \theta_i / \left| \boldsymbol{\theta}_{\mathtt{f}_j} \right|$, $\mu_j(1) = \sum_{i \in \mathtt{t}_j} y_i \, \theta_i / \left| \boldsymbol{\theta}_{\mathtt{t}_j} \right|$.

We could use the Bayesian bootstrap to simulate the posterior for σ_j implied by the exponential posterior on $\boldsymbol{\theta}$, but an analytic expression is not available. Instead, we follow the approach used in Lancaster (2003), Poirier (2011), and Taddy et al. (2014): derive a first-order Taylor approximation to the function σ_j and describe the posterior for that related functional.

In particular, the $1 \times n$ gradient of σ_j with respect to $\boldsymbol{\theta}$ is

$$\nabla \sigma_j^2 = \nabla \frac{1}{n} \left[\sum_i \theta_i y_i^2 - \frac{1}{|\boldsymbol{\theta}_{\mathtt{f}}|} \left(\mathbf{y}_{\mathtt{f}}' \boldsymbol{\theta}_{\mathtt{f}} \right)^2 - \frac{1}{|\boldsymbol{\theta}_{\mathtt{t}}|} \left(\mathbf{y}_{\mathtt{t}}' \boldsymbol{\theta}_{\mathtt{t}} \right)^2 \right] \tag{7}$$

which has elements $\nabla_i \sigma_j^2 = \left(y_i - \mu(x_{ij}) \right)^2 / n$

The Taylor approximation is then

$$\begin{aligned} \sigma_j^2 \approx \tilde{\sigma}_j^2 &= \sigma_j^2(\mathbf{1}) + \nabla \sigma^2 \big|_{\boldsymbol{\theta} = \mathbf{1}} (\boldsymbol{\theta} - \mathbf{1}) \\ &= \frac{1}{n} \sum_i \theta_i \left(y_i - \bar{y}_j(x_{ij}) \right)^2 \end{aligned} \tag{8}$$

with $\bar{y}_j(0) = \frac{1}{n_{\mathtt{f}_j}} \sum_{i \in \mathtt{f}_j} y_i$ and $\bar{y}_j(t) = \frac{1}{n_{\mathtt{t}_j}} \sum_{i \in \mathtt{t}_j} y_i$ the observed response averages in each partition.

Suppose that $\sigma_1(\mathbf{1}) < \sigma_j(\mathbf{1}) \; \forall j$, so that variable '1' is that selected for splitting based on the unweighted data sample. Then we can quantify variability about this selection by looking at differences in approximate impurity,

$$\begin{aligned} \Delta_j(\boldsymbol{\theta}) &= \tilde{\sigma}_1^2 - \tilde{\sigma}_j^2 \\ &= \frac{1}{n} \sum_i \theta_i \big[\bar{y}_1^2(x_{i1}) - \bar{y}_j^2(x_{ij}) - \\ &\qquad\qquad 2 y_i \left(\bar{y}_1(x_{i1}) - \bar{y}_j(x_{ij}) \right) \big] \\ &\equiv \frac{1}{n} \sum_i \theta_i d_{ji}. \end{aligned} \tag{9}$$

Say $\mathbf{d}_j = [d_{j1} \dots d_{jn}]'$ is the vector of squared error differences. Then the total difference has mean $\mathbb{E}\Delta_j = \bar{d}_j$ and variance $\mathrm{var}\Delta_j = \mathbf{d}_j' \mathbf{d}_j / n^2$. Since Δ_j is the mean of independent Exponential random variables with known means and variances, the central limit theorem applies and it converges in distribution to a Gaussian:

$$\sqrt{n}(\Delta_j(\boldsymbol{\theta}) - \bar{d}_j) \rightsquigarrow \mathrm{N}(0, \; \mathbf{d}_j' \mathbf{d}_j / n). \tag{10}$$

The weighted-sample impurity-minimizing split matches that for the unweighted-sample if and only if all Δ_j are negative, which occurs with probability (note $\bar{d}_j < 0$)

$$\begin{aligned} \mathrm{p}\left(\Delta_j < 0 : \; j = 2 \dots p \right) &\geq 1 - \sum_{j=2}^{p} \mathrm{p}(\Delta_j > 0) \\ &\rightsquigarrow 1 - \sum_{j=2}^{p} \Phi\left(- \frac{\sqrt{n} \left| \bar{d}_j \right|}{\sqrt{\mathbf{d}_j' \mathbf{d}_j / n}} \right) \\ &\geq 1 - \frac{1}{\sqrt{2\pi}} \sum_{j=2}^{p} \frac{\exp(-n z_j^2 / 2)}{z_j \sqrt{n}} \end{aligned} \tag{11}$$

where $z_j = \left| \bar{d}_j \right| \left(\mathbf{d}_j' \mathbf{d}_j / n \right)^{-\frac{1}{2}}$ is sample mean increase in impurity over the sample standard deviation of impurity. This ratio is bounded in probability, so that that the exponential bound goes to zero very quickly with n. In particular, ignoring variation in z_j across variables, we arrive at the approximate lower bound on the probability of the sample split

$$\mathrm{p}\left(\text{posterior split matches sample split} \right) \gtrsim 1 - \frac{p}{\sqrt{n}} e^{-n}.$$

Even allowing for $p \approx n \times d$, with d some underlying continuous variable dimension and p the input dimension discretization on these variables, the probability of the observed split goes to one at order $\mathcal{O}(n^{-1})$ if $d < e^n / n^{3/2}$.

Given this, why is there any uncertainty at all about trees? The answer is recursion: each split is conditionally stable given the sample at the current node, but the probability of any specific sequence of splits is roughly (we don't actually have independence) the product of individual node split probabilities. This will get small as we move deeper

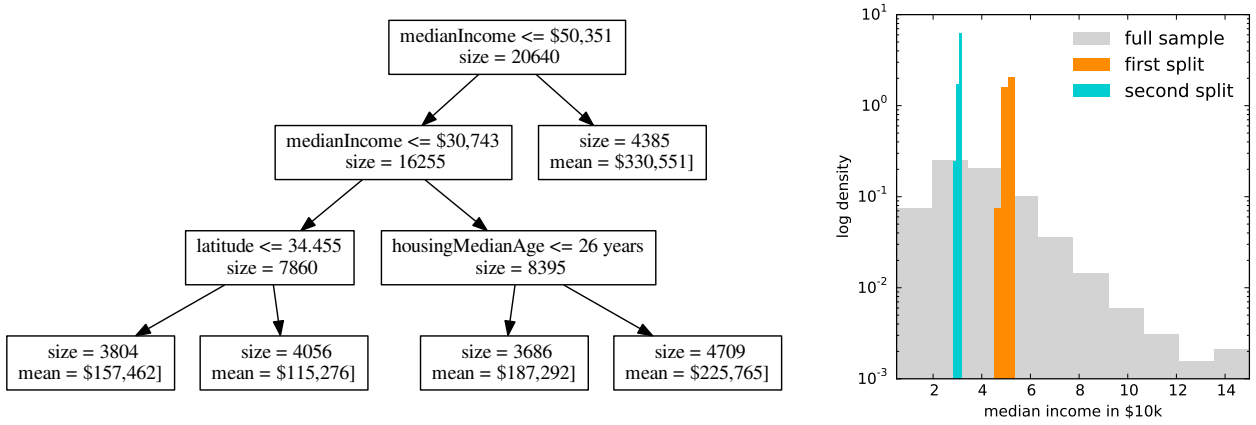

Figure 4. California housing data. The left shows the CART fit on unweighted data with a minimum of 3500 samples-per-leaf. The right panel shows the distribution of first and second split locations – always on median income – across 100 draws from the BF posterior.

down the tree, and given one split different from the sample CART the rest of the tree will grow arbitrarily far from this modal structure. In addition, the sample size going into our probability bounds is shrinking exponentially with each partition, whereas the dimension of eligible split variables is reduced only by one at each level.

Regardless of overall tree variability, we can take from this section an expectation that for large samples the high-level tree structure varies little across posterior DGP realizations. The next section shows this to be the case in practice.

3.2. Trunk stability in California

We'll illustrate the stability of high-level tree structure on our California housing data. Consider a 'trunk' DT fit to the unweighted data with no less than 3500 census blocks (out of 20640 total) in each leaf partition. This leads to the tree on the left of Figure 4 with five terminal nodes. It splits on the obvious variable of median income, and also manages to divide California into its north and south regions (34.455 degrees north is just north of Santa Barbara).

To investigate tree uncertainty, we can apply the BF algorithm and repeatedly fit similar CART trees to randomly-weighted data. Running a 100 tree BF, we find that the sample tree occurs 62% of the time. The second most common tree, occurring 28% of the time, differs only in that it splits on median income again instead of on housing median age. Thus 90% of the posterior weight is on trees that split on income twice, and then latitude. Moreover, a striking 100% of trees have first two splits on median income. From this, we can produce the plot in the right panel of Figure 4 showing the locations of these first two splits: each split-location posterior is tightly concentrated around the corresponding sample CART split.

Given such trunk stability after only 20k observations, we have hope for much deeper tree stability under the 1-100 million+ observation datasets encountered when analyzing internet transaction data.

4. Empirical Bayesian forests

Empirical Bayes (EB) is an established framework with a successful track record in fast approximate Bayesian inference; see, e.g., Efron (2010) for an overview. In parametric models, EB can be interpreted as fixing at their marginal posterior maximum (MAP) the parameters at higher levels of a hierarchical model. For example, in the simple setting of many group means (the average student test score for each of many schools) shrunk to a global center (the outcome for an imaginary 'average school'), an EB procedure will shrink each group mean toward the overall sample average (each school towards all-student average). Kass & Steffey (1989) investigate such procedures and show that, under fairly general conditions, the EB conditional posterior for each group mean quickly approaches the fully Bayesian unconditional posterior as the sample size grows. *This occurs because there is little uncertainty about the global mean.*

CART trees are not a parametric model, but they are hierarchical and admit an interpretation similar to those studied in Kass & Steffey (1989). The data which reaches any given interior node is a function of the partitioning implied by nodes shallower in the tree. Moreover, due to the greedy algorithm through which CART grows, a given shallow trunk is unaffected by changes to the tree structure below. Finally, Section 3 demonstrated that, like high levels in a parametric hierarchical model, there is relatively little uncertainty about high levels of the tree.

An empirical Bayesian forest (EBF) takes advantage of this structure by fixing the highest levels in the hierarchy – the

earliest CART splits – at a single estimate of high posterior probability. In particular, we fit a single shallow CART *trunk* to the unweighted sample data, and then sample a BF ensemble of *branches* at each terminal node of this trunk. The initial CART trunk thus maps observations to their branch, and each branch BF deals with a dataset of manageable size and can be fit in parallel without any communication with the other branches. That is, EBF replaces the BF posterior sample of trees with a conditional posterior sample that takes the pre-fit trunk as fixed. Since the trunk has relatively low variance for large samples (precisely the setting where such distribution is desirable), the EBF should provide predictions similar to that of the full BF at a fraction of the cost.

In contrast, consider the 'sub-sample forest' (SSF) algorithm, which replaces the full data with random subsamples of manageable size. Independent forests are fit to each sub-sample and predictions are averaged across all forests. SSF is a commonly applied strategy (e.g., see mention, but not recommendation, of it in Panda et al., 2009), but it implies using only partial data for learning deep tree structure. Although the tree trunks are stable, the full tree is highly uncertain and learning such structure is precisely where you want to use a full Big Data sample.

4.1. Out-of-sample experiments

In the California housing experiment of Figure 3 and Table 4, EBF[10] predictions are only 2% worse than those from the full BF. In contrast, SSF predictions are 10% worse.

We consider two additional prediction problems. The first example, taken from (Cortez et al., 1998), involves prediction of an 'expert' quality ranking on the scale of 0-10 for wine based upon 11 continuous attributes (physiochemical properties of the wine) plus wine color (red or white). There are 4898 observations. Results are in Figure 5: EBF is only 1% worse than the full BF, while SSF is 12% worse.

The second example is from the Nielson Consumer Panel data, and our sample contains 73,128 purchases of light beer in a number of US markets from during 2004. The response of interest is brand choice, of a possible five major light beer labels. Each purchase is associated with a household that is codified through 16 standard demographic categorical variables (maximum age, total income, main occupation, etc). Applying classification forests and DTs[11] leads to the results in Figure 6: EBF is only 4.4% worse than the BF, while SSF is 38% worse.

[10]EBFs use five node trunks in this Section. The SSFs are fit on data split into five equally sized subsets.

[11]based on Gini impurity minimization

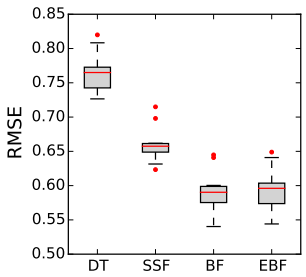

$\overline{\text{RMSE}}$	% WTB	
0.5905	0.0	BF
0.5953	0.8	EBF
0.6607	11.9	SSF
0.7648	29.5	DT

Figure 5. Wine Data: 10-fold OOS prediction experiment Root Mean Square Error and % Worse than Best for the mean RMSE.

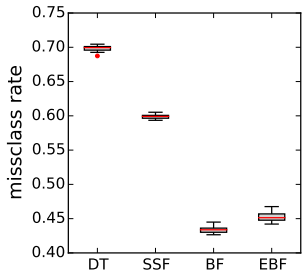

$\overline{\text{MCR}}$	% WTB	
0.4341	0.0	BF
0.4531	4.4	EBF
0.5989	38.0	SSF
0.6979	60.8	DT

Figure 6. Beer Data: 10-fold OOS prediction experiment Miss-Classification Rate and % Worse than Best for the average MCR.

4.2. Scaling for Big Data

To close, we note that this work is motivated by the need for reliable forest fitting algorithms that can be deployed on millions or hundreds of millions of observations, as encountered when analyzing internet commerce data. A number of additional engineering details are required for such deployment, but the basic approach is straight forward: an initial trunk is fit (possibly to a data subset)[12], and this trunk then acts as a sorting function to map observations to separate locations corresponding to each branch. Forests are then fit at each location for each branch.

Preliminary work at eBay.com applies EBFs for prediction of of 'Bad Buyer Experiences' (e.g. complaints, returns, or shipping problems) on the site. Training on a relatively small sample of 12 million transactions, the EBF algorithm using 32 branch chunks is able to provide a 1.3% drop in misclassification over the SSF alternatives. This amounts to more than 20,000 extra detected BBE occurrences over the short sample window, potentially giving eBay the opportunity to contact those buyers and attempt to fix the problems or even stop them before they occur.

[12]Note that the original trunk fit can itself be fit in distribution, e.g. using the `MLLib` library for Apache Spark.

References

Appel, Ron, Fuchs, Thomas, Dollr, Piotr, and Perona, Pietro. Quickly boosting decision trees-pruning underachieving features early. In *JMLR Workshop and Conference Proceedings*, volume 28, pp. 594–602. JMLR, 2013.

Breiman, Leo. Random forests. *Machine Learning*, 45: 5–32, 2001.

Breiman, Leo, Friedman, Jerome, Olshen, Richard, and Stone, Charles. *Classification and regression trees*. Chapman & Hall/CRC, 1984.

Chamberlain, Gary and Imbens, Guido W. Nonparametric applications of bayesian inference. *Journal of Business & Economic Statistics*, 21:12–18, 2003.

Chipman, H.A., George, E.I., and McCulloch, R.E. Bayesian CART model search (with discussion). *Journal of the American Statistical Association*, 93:935–960, 1998.

Chipman, Hugh A., George, Edward I., and McCulloch, Robert E. BART: Bayesian additive regression trees. *The Annals of Applied Statistics*, 4:266–298, 2010.

Clyde, Merlise and Lee, Herbert. Bagging and the bayesian bootstrap. In *Artificial Intelligence and Statistics*, 2001.

Cortez, P., Cerdeira, A., Almeida, F., Matos, T., and Reis, J. Modeling wine preferences by data mining from physicochemical properties. *Decision Support Systems*, 47(4): 547–553, 1998.

Efron, Bradley. *Large-Scale Inference: Empirical Bayes Methods for Estimation, Testing, and Prediction*. IMS Statistics Monographs. Cambridge, 2010.

Ferguson, T.S. A bayesian analysis of some nonparametric problems. *Annals of Statistics*, 1:209–230, 1973.

Friedman, Jerome. Multivariate adaptive regression splines. *The Annals of Statistics*, 19:1–67, 1991.

Geurts, Pierre and Wehenkel, Louis. Investigation and reduction of discretization variance in decision tree induction. In *Machine Learning: ECML 2000*, pp. 162–170. Springer, 2000.

Geurts, Pierre, Ernst, Damien, and Wehenkel, Louis. Extremely randomized trees. *Machine Learning*, 63:3–42, 2006.

Gramacy, Robert B. and Lee, Herbert K. H. Bayesian treed gaussian process models with an application to computer modeling. *Journal of the American Statistical Association*, 103:1119–1130, 2008.

Hollander, Myles and Wolfe, Douglas. *Nonparametric Statistical Methods*. Wiley, 2nd edition, 1999.

Hothorn, Torsten, Hornik, Kurt, and Zeileis, Achim. Unbiased recursive partitioning: A conditional inference framework. *Journal of Computational and Graphical Statistics*, 15:651–674, 2006.

Kass, G. V. An exploratory technique for investigating large quantities of categorical data. *Applied Statistics*, 29:119–127, 1980.

Kass, Robert E. and Steffey, Duane. Approximate bayesian inference in conditionally independent hierarchical models (parametric empirical bayes models). *Journal of the American Statistical Association*, 84:717, 1989. ISSN 01621459.

Lancaster, Tony. A note on bootstraps and robustness. Technical report, Working Paper, Brown University, Department of Economics, 2003.

Loh, Wei-Yin. Regression trees with unbiased variable selection and interaction detection. *Statistica Sinica*, 12: 361–386, 2002.

Pace, R. Kelley and Barry, Ronald. Sparse spatial autoregressions. *Statistics and Probability Letters*, 33:291–297, 1997.

Panda, Biswanath, Herbach, Joshua S., Basu, Sugato, and Bayardo, Roberto J. Planet: massively parallel learning of tree ensembles with mapreduce. *Proceedings of the VLDB Endowment*, 2(2):1426–1437, 2009.

Pedregosa, F., Varoquaux, G., Gramfort, A., Michel, V., Thirion, B., Grisel, O., Blondel, M., Prettenhofer, P., Weiss, R., Dubourg, V., Vanderplas, J., Passos, A., Cournapeau, D., Brucher, M., Perrot, M., and Duchesnay, E. Scikit-learn: Machine learning in Python. *Journal of Machine Learning Research*, 12:2825–2830, 2011.

Poirier, Dale J. Bayesian interpretations of heteroskedastic consistent covariance estimators using the informed bayesian bootstrap. *Econometric Reviews*, 30(4):457–468, 2011.

Rubin, Donald. The bayesian bootstrap. *The Annals of Statistics*, 9:130–134, 1981.

Taddy, M. A., Gramacy, R. B., and Polson, N. G. Dynamic trees for learning and design. *Journal of the American Statistical Association*, 106:109–123, 2011.

Taddy, Matt, Gardner, Matt, Chen, Liyun, and Draper, David. Heterogeneous treatment effects in digital experimentation. *arXiv preprint arXiv:1412.8563*, 2014.

Venables, W. N. and Ripley, B. D. *Modern Applied Statistics with S*. Springer, New York, fourth edition, 2002.